International Journal of Pharmaceutics 374 (2009) 53–57

Contents lists available at ScienceDirect

International Journal of Pharmaceutics

journal homepage: www.elsevier.com/locate/ijpharm

Montmorillonite as a drug delivery system: Intercalation and in vitro release of timolol maleate

Ghanshyam V. Joshi [a], Bhavesh D. Kevadiya [a], Hasmukh A. Patel [a], Hari C. Bajaj [a,*], Raksh V. Jasra [b]

[a] Discipline of Inorganic Materials and Catalysis, Central Salt and Marine Chemicals Research Institute (CSMCRI), Council of Scientific and Industrial Research (CSIR), Gijubhai Badheka Marg, Bhavnagar - 364 002, Gujarat, India
[b] R & D Centre, Reliance Industries Limited, Vadodara Manufacturing Division, Vadodara - 391 346, Gujarat, India

ARTICLE INFO

Article history:
Received 6 January 2009
Received in revised form 3 March 2009
Accepted 6 March 2009
Available online 19 March 2009

Keywords:
Timolol maleate
Montmorillonite
Intercalation
Control release

ABSTRACT

The need for safe, therapeutically effective, and patient-compliant drug delivery systems continuously leads researchers to design novel tools and strategies. Clay minerals play a very crucial role in modulating drug delivery. This work examines the advantageous effect of clay mineral as drug carrier for timolol maleate (TM), a nonselective β-adrenergic blocking agent. The intercalation of TM into the interlayer of montmorillonite (MMT) at different pH and initial concentration is demonstrated. MMT–TM hybrid was characterized by X-ray diffraction (XRD), Fourier transformed infrared (FT-IR), and thermal analysis (TG-DTA). TM was successfully intercalated into the interlayer of MMT, and in vitro release properties of the intercalated TM have been investigated in simulated gastric fluid (pH 1.2) and simulated intestinal fluid (pH 7.4) at 37 ± 0.5 °C. Controlled release of TM from MMT–TM hybrid has been observed during in vitro release experiments.

1. Introduction

Timolol maleate (TM), S-(−)-1-[(*tert*-butylamino)-3-(4-morpholino-1,2,5-thiadiazol-3-yl)oxy]-2-propanol maleate (Fig. 1) is a nonselective β-adrenergic blocking agent. Timolol is effective against hypertension, arrhythmias, and angina pectoris, as well as for the secondary prevention of myocardial infarction (Turkdemir et al., 2001).

Montmorillonite (MMT) clay is one of the smectite group, composed of silica tetrahedral sheets layered between an alumina octahedral sheets. The imperfection of the crystal lattice and the isomorphous substitution induce a net negative charge that leads to the adsorption of alkaline earth metal ions in the interlayer space. Such imperfection is responsible for the activity and exchange reactions with organic compounds. MMT also contains dangling hydroxyl end-groups on the surfaces (Khalil et al., 2005). MMT has large specific surface area; exhibits good adsorb ability, cation exchange capacity, standout adhesive ability, and drug-carrying capability. Thus, MMT is a common ingredient as both the excipient and active substance in pharmaceutical products (Wang et al., 2008). The intercalation of organic species into layered inorganic solids provides a useful and convenient route to prepare organic–inorganic hybrids that contain properties of both the inorganic host and organic guest in a single material (Mohanambe and Vasudevan, 2005).

In recent years, smectite clays intercalated by drug molecules have attracted great interest from researchers since they exhibit novel physical and chemical properties. Zheng et al. (2007) have investigated the intercalation of ibuprofen into MMT as a sustained release drug carrier. Lin et al. (2002) studied the intercalation of 5-fluorouracil with MMT as drug carrier. Fejer et al. (2001) reported intercalation and release behavior of promethazine chloride and buformin hydrochloride from MMT. Nunes et al. (2007) studied the loading and delivery of sertraline using MMT K10. Dong and Feng (2005) synthesized the poly(D,L-lactide-co-glycolide)-MMT nanoparticles by the emulsion/solvent evaporation method for oral delivery of paclitaxel.

The present paper focused on the intercalation of TM into the interlayer of MMT under different reaction conditions, such as pH and initial concentration of TM. The MMT–TM hybrid was characterized by XRD, FT-IR, and TG-DTA. Release profile of TM from MMT–TM hybrid was carried out by taking TM encapsulated in MMT in the dialysis membrane tubing, and the dialysis bag was suspended in 500 ml vessel containing 300 ml simulated gastric and intestinal fluid.

2. Experimental

2.1. Materials

Timolol maleate was purchased from Sigma–Aldrich, USA. HCl, KCl, KH_2PO_4, NaCl, and NaOH were purchased from S. D. Fine Chem-

* Corresponding author. Tel.: +91 278 2471793; fax: +91 278 2567562.
E-mail address: hcbajaj@csmcri.org (H.C. Bajaj).

0378-5173/$ – see front matter © 2009 Published by Elsevier B.V.
doi:10.1016/j.ijpharm.2009.03.004

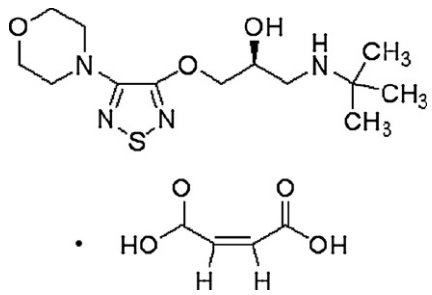

Fig. 1. Chemical structure of timolol maleate.

icals, India and were used as received. The MMT rich bentonite clay was collected from Akli mines, Barmer district, Rajasthan, India. De-ionized water was obtained from Milli-Q Gradient A10 water purification system.

2.2. Purification of MMT

To obtain MMT in Na-form, 300 g of raw bentonite was dispersed in 3 l of 0.1 M NaCl solution, stirred for 12 h and centrifuged. The above procedure was repeated thrice. Finally, the slurry was centrifuged and washed with de-ionized water until free from chloride ion as tested by $AgNO_3$ solution (Bergaya et al., 2006). Na-MMT was purified by sedimentation technique as described earlier (Patel et al., 2007a), according to the Stokes law of sedimentation. The purified MMT was obtained by dispersing 150 g of Na-MMT in 10 l de-ionized water and collecting the supernatant dispersion of particles <2 μm after the pre-calculated time (10 h) and height (15 cm) at 30 °C. The Na-MMT slurry was dried at 100 °C and ground to pass through 200 mesh sieve (ASTM). The cation exchange capacity (CEC) of MMT was measured by the standard ammonium acetate method at pH 7 (Bergaya et al., 2006), and was 91 mequiv./100 g of MMT on dry basis (dried at 110 °C).

2.3. Intercalation kinetics

The experiments were performed to optimize the time required for maximum intercalation of TM into the interlayer of MMT. 30 ml aqueous solution of TM containing 31 mg of TM was mixed with 100 mg of MMT powder for 1, 3, 7, 9, and 15 h at 30 °C in a 100 ml conical flask with continuous stirring. The reaction mixtures were filtered and concentration of TM in the filtrate was determined by UV–vis spectroscopy at λ_{max} = 294 nm.

2.4. Effect of pH

The experiments were performed to determine the optimum pH for intercalation of TM into the interlayer of MMT. For this purpose, TM and MMT mixture were treated at different pH at constant temperature, time, and concentration. 30 ml aqueous solution of TM containing 31 mg of TM was mixed with 100 mg of MMT powder at pH 2.2, 3.2, 4.4, 5.7, 7, 8.5, and 10.8 for optimized time of 1 h at 30 °C in a 100 ml conical flask with continuous stirring. The reaction mixtures were filtered and concentration of TM in the filtrate was determined by UV–vis spectroscopy at λ_{max} = 294 nm.

2.5. Initial TM concentration

To achieve maximum intercalation of TM into MMT, reactions were carried out at different initial concentration of TM at constant temperature, time, and pH. 30 ml aqueous solution of TM containing different initial amount of TM (5.1, 10.3, 15.5, 20.6, 25.7, 31.0, 42.0, 52.5, and 63 mg) were treated with 100 mg of MMT powder for 1 h at pH 5.7 at 30 °C in a 100 ml conical flask with continuous stirring. The reaction mixtures were filtered and concentration of TM in the filtrate was determined by UV–vis spectroscopy at λ_{max} = 294 nm.

2.6. Characterization

X-ray diffraction (XRD) analysis was carried out with a Phillips powder diffractometer X' Pert MPD using PW3123/00 curved Ni-filtered Cu Kα (λ = 1.54056 Å) radiation with slow scan of 0.3°/s in 2θ range of 2–10°. Fourier transform infrared spectra (FT-IR) were measured with PerkinElmer, GX-FTIR as KBr pellet. Thermogravimetric analysis was carried out within 30–800 °C at the rate 10 °C/min in the nitrogen flow using Mettler-Toledo, TGA/SDTA 851e. UV–vis absorbance of TM solutions were measured using UV–vis spectrophotometer (Cary 500, Varian) equipped with a quartz cell having a path length of 1 cm. Release experiments were performed using Julabo shaking water bath (SW23).

2.7. Release of TM from MMT–TM hybrid

Buffer solution of pH 1.2 (simulated gastric fluid) was prepared by mixing 250 ml of 0.2 M HCl and 147 ml of 0.2 M KCl. Buffer solution of pH 7.4 (simulated intestinal fluid) was prepared by mixing 250 ml of 0.1 M KH_2PO_4 and 195.5 ml of 0.1 M NaOH. In vitro release studies were carried out in phosphate buffered saline media of pH 7.4 and simulated gastric fluid at pH 1.2 using the dialysis bag technique (Marchal-Heussler et al., 1990). Dialysis sacs were equilibrated with the dissolution medium for a few hours prior to experiments. 150 mg of MMT–TM hybrid in 5 ml of buffer solution was taken in the dialysis bag. Dialysis bag was dipped into receptor compartment containing 300 ml dissolution medium, which was shaked at 37 ± 0.5 °C in Julabo shaking water bath (SW23). The receptor compartment was closed to prevent the evaporation losses from the dissolution medium. The shaking frequency was kept at 100 rpm. 5 ml of sample was withdrawn at regular time intervals and the same volume was replaced with a fresh dissolution medium. Samples were analyzed for TM content by UV spectrophotometer at λ_{max} = 294 nm. These studies were performed in triplicate for each sample and the average values were used in data analysis.

3. Results and discussion

3.1. Intercalation kinetics

Intercalation of TM in MMT is very rapid process, due to occurrence of ion-exchange reaction between the interlayer Na^+ ions and cationic TM molecules. 17% of TM was intercalated within 1 h of interaction time, which remained constant up to 15 h. Therefore, interaction time was set to 1 h to avoid the partial intercalation in the subsequent experiments.

3.2. Intercalation at different pH values

Fig. 2 shows the effect of pH on the intercalation of TM into the interlayer of MMT. The results of pH effect on the intercalation of TM in MMT in the pH range 3.2–8.5 were suggesting that intercalation of TM remains almost constant within experimental error. There was a sharp decrease in intercalation of TM in MMT, when the pH was above 8.5 and below 3.2. This can be explained based on pK_a value of TM. The pK_a of TM is ~9.4 (Martıĭnez et al., 2000; Kanikkannana et al., 2001), which implies that at pH ≤ 7.4, the TM exists as mono charged cations due to protonation of the amine. Intercalation at pH 10.8 is only about 3.2%, due to largely uncharged

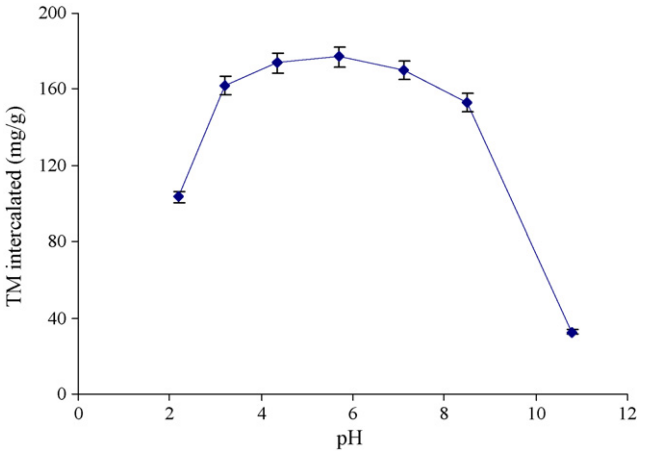

Fig. 2. Effect of pH on interaction of TM into MMT (MMT = 100 mg/30 ml, TM = 31 mg, temperature = 30 °C, time = 1 h).

TM species. Below pH 3.2, there is a decrease in adsorption of TM in the clay lattice. This is due to the competition between the cationic drug and H^+ protons, which exist on the MMT surface at low pH value as the silanol groups on the clay surface get protonated (Seki and Kadir, 2006).

3.3. Effect of initial TM concentration on its intercalation in clay

The intercalation of TM in MMT is affected by the initial TM concentration (Fig. 3). As the initial concentration of TM in the solution increases, the amount of intercalation increases may be due to greater concentration gradient at the initial stage. However, it reached equilibrium after intercalation of 217 mg of TM/g of MMT.

3.4. XRD, FT-IR and thermal analysis

Fig. 4 shows the XRD pattern of MMT and MMT–TM hybrid prepared under optimized conditions. The characteristic 2θ peak of (0 0 1) plane for MMT and MMT–TM hybrid is observed at 7.4° and 5.98°, with basal spacing of 1.18 and 1.47 nm, respectively. According to the Bragg's law, the peak shifting from higher diffraction angle to lower diffraction angle is due to increase in the d-spacing which indicates that TM has been effectively intercalated into the interlayer of MMT (Scheme 1) and is lying flat on the surface of MMT as monolayer (Lagaly and Dekany, 2005).

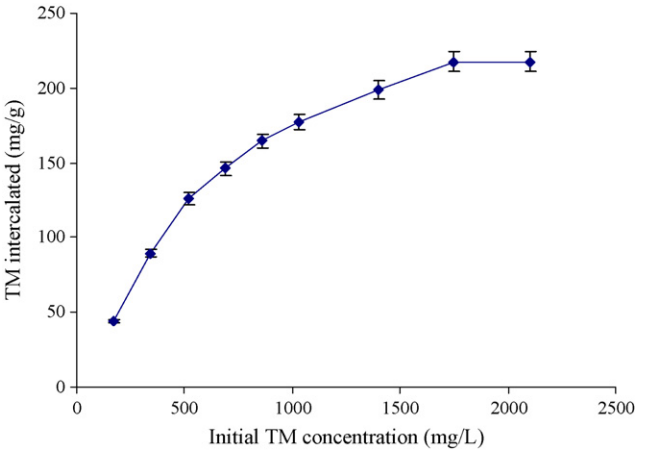

Fig. 3. Effect of initial concentration of TM on intercalation (MMT = 100 mg/30 ml, pH 5.7, temperature = 30 °C, time = 1 h).

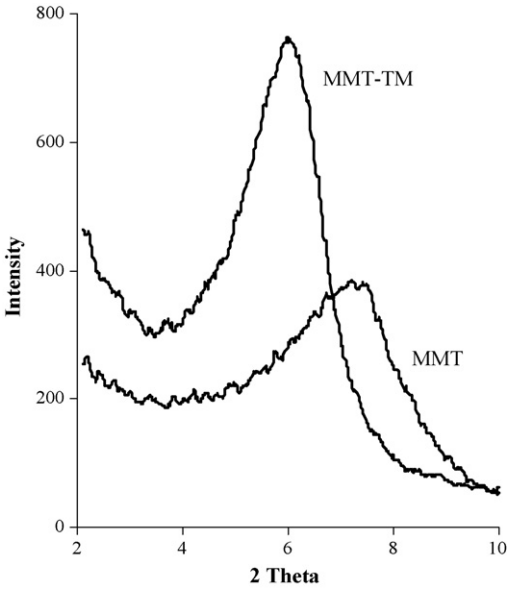

Fig. 4. XRD patterns of MMT and MMT–TM hybrid.

Fig. 5 depicts the FT-IR spectra of MMT, TM, and MMT–TM hybrid. MMT shows the characteristic absorption bands at 3400 cm^{-1} due to –OH stretching band for adsorbed water. The bands at 3620 and 3698 cm^{-1} are due to –OH band stretch for Al–OH and Si–OH. The shoulders and broadness of the structural –OH band are mainly due to contributions of several structural –OH groups occurring in the MMT. The overlaid absorption peak at 1640 cm^{-1} is attributed to –OH bending mode of adsorbed water. The characteristic peak at 1115 and 1035 cm^{-1} is due to Si–O stretching (out-of-plane) and Si–O stretching (in-plane) vibration for layered silicates, respectively. Peaks at 915, 875, and 836 cm^{-1} are attributed to AlAlOH, AlFeOH, and AlMgOH bending vibrations, respectively (Patel et al., 2007b). TM showed a broad band appearing at 3328 cm^{-1} due to O–H/N–H stretching vibrations. The bands at 2970, 2898, and 2853 cm^{-1} are due to aliphatic C–H stretching vibrations. Acid carbonyl group of maleic acid and N–H bending vibrations gave band at 1710 and 1500 cm^{-1}. The C=N stretching vibrations appears at 1620 cm^{-1}. Bands at 1262 and 1119 cm^{-1} are due to the =C—O—C and morpholino C–O–C stretching vibrations, respectively, while the bands at 1230 and 953 cm^{-1} are due to O–H bending and hydroxyl C–O stretching vibrations, respectively

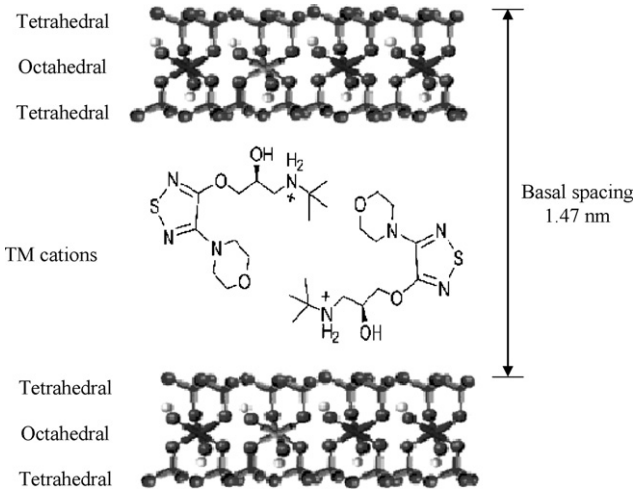

Scheme 1. Possible structural arrangement of MMT–TM.

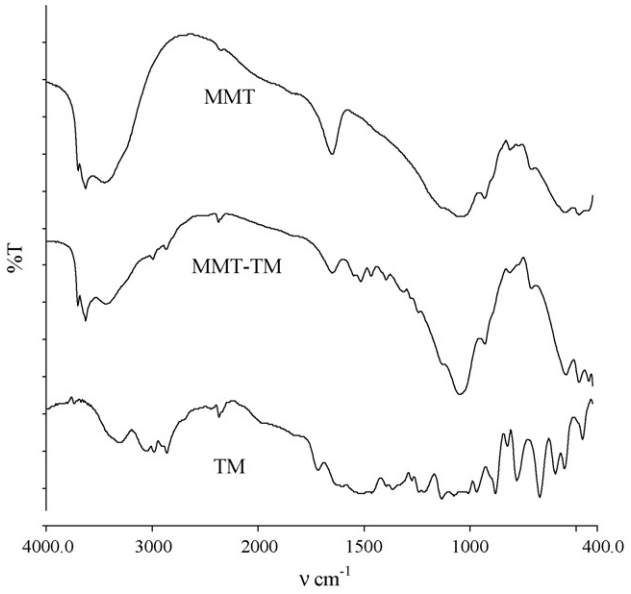

Fig. 5. FT-IR of MMT–TM, MMT, and TM.

(Agnihotri and Aminabhavi, 2007). In the IR spectra of MMT–TM hybrid, not only characteristic bands belonging to MMT and TM appear in the spectrum but also several new absorption bands appears at 1300, 1383, and 1454 cm^{-1} which indicates that TM interacts strongly with the MMT layers.

Fig. 6A and B depict the TGA and DTA profile for MMT–TM, MMT, and pristine TM. Two major weight loss patterns were observed in the temperature range of 80–100 and 600–750 °C for MMT. The first weight loss corresponds to evaporation of adsorbed water, which is resulted in a strong endothermic peak at 100 °C. The second prominent weight loss was observed at 600–750 °C due to the loss of structural hydroxyl group (Patel et al., 2007a). Pristine TM shows a sharp weight loss at around 180–350 °C, resulting in strong endothermic peak at this temperature. MMT–TM hybrid shows weight loss in three steps in the temperature region of 80–100, 200–300, and 600–750 °C. It is explicable that decomposition of intercalated TM took place in the temperature range of 200–350 °C. A weight loss at 100 and 650 °C is due to loss of water and structural hydroxyl group in the MMT–TM hybrids, respectively.

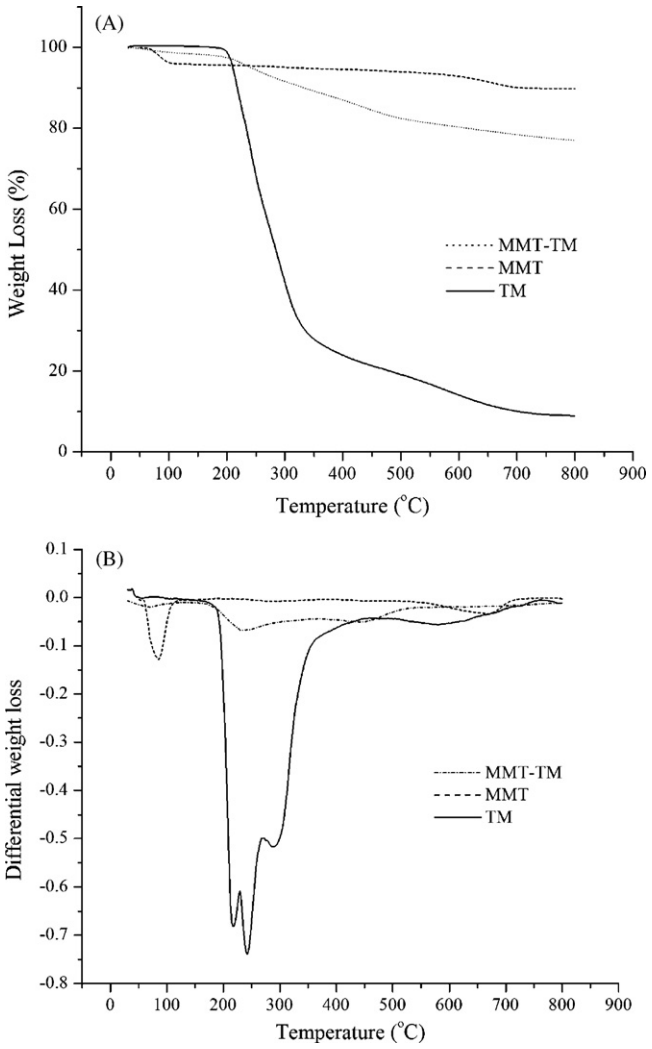

Fig. 6. TGA (A) and DTA (B) curve of MMT–TM, MMT, and TM.

Moreover, the existence of electrostatic interactions between the protonated amino groups of the TM cations and the anionic charges at surface of the MMT may leads to incomplete release (Nunes et al., 2007).

3.5. Release profiles

The controlled release tests were carried out by suspending the MMT–TM hybrid in simulated gastric and intestinal fluids under continuous shaking at 37 ± 0.5 °C. TM released from MMT–TM hybrid was measured at 30 min of time intervals by measuring the absorbance at λ = 294 nm (Fig. 7). The release of TM from the MMT–TM hybrid is slow and persistent in simulated gastric (pH 1.2) as well as in intestinal (pH 7.4) fluids. 14, 31, 39, and 43% of TM was released after 0.5, 2, 4, and 9 h, respectively at pH 1.2 and 17, 32, 43, and 48% of TM was released after 0.5, 2, 4, and 9 h, at pH 7.4, respectively. This slow and sustained release process may be interpreted based on the ion-exchange process between the intercalated drug and the alkali metal ions of the buffer (Zhang et al., 2006). The maximum release of TM from MMT–TM hybrids in both gastric and intestinal fluids was observed to be in the range 43–48%. Based on the release profiles at pH 1.2 and 7.4, the equilibrium percentage released of TM was not up to 100%. This is probably due to the characteristic of ion-exchange reaction, i.e. this is an equilibrium process, and the interlayer cations cannot be exchanged completely.

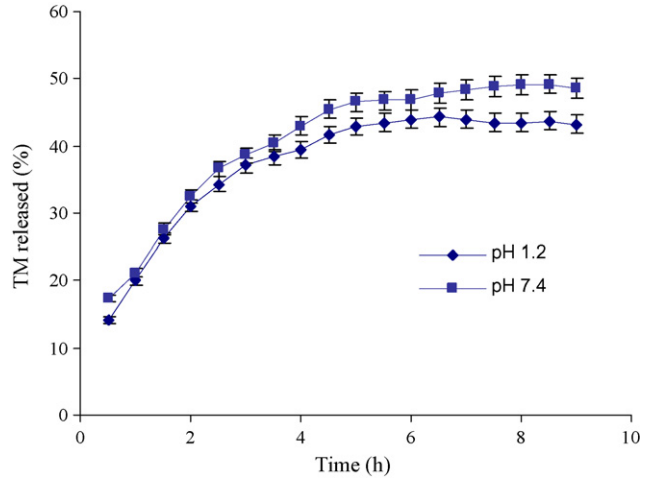

Fig. 7. Release profile of TM from the MMT–TM hybrid in simulated gastric fluid (pH 1.2) and simulated intestinal fluid (pH 7.4) at 37 ± 0.5 °C.

4. Conclusion

In summary, we have shown the intercalation of TM into MMT and in vitro release of TM from MMT–TM hybrid. The intercalation of TM into MMT was rapid process and equilibrium was attained within 1 h. The maximum amount of TM intercalated into MMT is 217 mg/g MMT within 1 h at pH 5.7 and 30 °C. Intercalation of TM into MMT depends on the pH of the interaction medium. XRD patterns of hybrid material shows an increase in the d-spacing, conforming the intercalation of TM into the interlayer of MMT. TG-DTA of MMT–TM shows a sharp weight loss at about 200 °C due to decomposition of exchanged TM. In vitro release study showed that about 43 and 48% of TM was released from MMT–TM hybrid in simulated gastric fluid (pH 1.2) and intestinal fluid (pH 7.4), respectively. These studies indicate that MMT can be used as the sustained release carrier of TM in oral administration.

Acknowledgements

We are thankful to Council of Scientific and Industrial Research (CSIR) for funding under Network Project: NWP 0010; to Dr. P. Bhatt (XRD), Mr. V. Agarwal (FT-IR) and Mrs. Sheetal Patel (TGA) of the analytical section of the institute.

References

Agnihotri, S.A., Aminabhavi, T.M., 2007. Chitosan nanoparticles for prolonged delivery of timolol maleate. Drug Dev. Ind. Pharm. 33, 1254–1262.

Bergaya, F., Theng, B.K.G., Lagaly, G., 2006. Handbook of Clay Science, 1st edition. Elsevier Publication, Amsterdam.

Dong, Y., Feng, S.S., 2005. Poly (D,L-lactide-co-glycolide)/montmorillonite nanoparticles for oral delivery of anticancer drugs. Biomaterials 26, 6068.

Fejer, I., Kata, M., Eros, I., Berkesi, O., Dekani, I., 2001. Release of cationic drugs from loaded clay minerals. Colloid Polym. Sci. 279, 1177.

Kanikkannana, N., Singh, J., Ramaraoc, P., 2001. In vitro transdermal iontophoretic transport of timolol maleate: effect of age and species. J. Controll. Release 71, 99–105.

Khalil, H., Mahajan, D., Rafailovich, M., 2005. Polymer–montmorillonite clay nanocomposites. Part 1: complexation of montmorillonite clay with a vinyl monomer. Polym. Int. 54, 423–427.

Lagaly, G.T., Dekany, I., 2005. Adsorption on hydrophobized surfaces: clusters and self-organization. Adv. Colloid Interf. Sci. 114–115, 189–204.

Lin, F.H., Lee, Y.H., Jian, C.H., Wong, J.M., Shieh, M.J., Wang, C.Y., 2002. A study of purified montmorillonite intercalated with 5-fluorouracil as drug carrier. Biomaterials 23, 1981.

Marchal-Heussler, I., Maincent, P., Hoffman, M., Spittler, J., Couvreur, P., 1990. Antiglaucomatous activity of betaxolol chlorhydrate sorbed onto different isobutyl cyanoacrylate nanoparticle preparations. Int. J. Pharm. 58, 115–122.

Martıĭnez, V., Maguregui, M.I., Jimeĭnez, R.M., Alonso, R.M., 2000. Determination of the pK_a values of β-blockers by automated potentiometric titrations. J. Pharm. Biomed. Anal. 23, 459–468.

Mohanambe, L., Vasudevan, S., 2005. Anionic clays containing anti-inflammatory drug molecules: comparison of molecular dynamics simulation and measurements. J. Phys. Chem. B 109, 15651–15658.

Nunes, C.D., Vaz, P.D., Fernandes, A.C., Ferreira, P., Roma, C.C., Calhorda, M.J., 2007. Loading and delivery of sertraline using inorganic micro and mesoporous materials. Eur. J. Pharm. Biopharm. 66, 357.

Patel, H.A., Somani, R.S., Bajaj, H.C., Jasra, R.V., 2007a. Synthesis and characterization of organic bentonite using Gujarat and Rajasthan clays. Curr. Sci. 92, 1004.

Patel, H.A., Somani, R.S., Bajaj, H.C., Jasra, R.V., 2007b. Preparation and characterization of phosphonium montmorillonite with enhanced thermal stability. Appl. Clay Sci. 35, 194.

Seki, Y.S., Kadir, Y.C., 2006. Adsorption of promethazine hydrochloride with KSF montmorillonite. Adsorption 12, 89.

Turkdemir, M.H., Erdögdu, G., Aydemir, T., Karagözler, A.A., Karagözler, A.E., 2001. Voltammetric determination of timolol maleate: a β-adrenergic blocking agent. J. Anal. Chem. 56, 1047–1050.

Wang, X., Du1, Y., Luo, J., 2008. Biopolymer/montmorillonite nanocomposite: preparation, drug-controlled release property and cytotoxicity. Nanotechnology 19, 065707.

Zhang, H., Zou, K., Guo, S., Duan, X., 2006. Nanostructural drug–inorganic clay composites: structure, thermal property and in vitro release of captopril-intercalated Mg–Al-layered double hydroxides. J. Solid State Chem. 179, 1792–1801.

Zheng, J.P., Luan, L., Wang, H.Y., Xi, L.F., Yao, K.D., 2007. Study on ibuprofen/montmorillonite intercalation composites as drug release system. Appl. Clay Sci. 36, 297.